

A Surface Micromachined Microtactile Sensor Array *

Bonnie L. Gray
Department of ECE
University of California
Davis, CA 95616

Ronald S. Fearing
Department of EECS
University of California
Berkeley, CA 94720

Abstract

This paper discusses the design and testing of an eight-by-eight tactile capacitive array sensor for detection of sub-millimeter features and objects, where the entire sensor array is smaller than normal human spatial resolution of 1mm. Each square tactel is less than 100 μ m on a side, with similar spacing between elements. The structural material was doped polysilicon with an air gap dielectric of 0.5 μ m. A thin (50-80 μ m) protective layer of silicone rubber was adhered to the polysilicon surface of the sensor to provide interpolation of normal loads between elements. The sensors were tested and possessed good spatial uniformity, the capability of detecting millinewton forces, and good interpolation between elements. The sensors had severe hysteresis problems, but no detectable proximity effects.

1 Introduction

Most capacitive array sensors to date are designed for macroscopic robotics applications. Even designs utilizing micromachining for construction are often designed according to macroscale specifications and intended for macroscale use. Similarly, sensors designed for small feature perception are usually intended for use on systems much larger than the features they sense.

We propose a sensor design for experimentation in medium-density sub-millimeter tactile sensing, where the entire tactile array is smaller than 1mm² and spatial resolution is at least ten times that of a human. Several potential uses for such a sensor would exploit its small size and high resolution. One use is placement on the end of a catheter or on the fingers of an endoscopic-surgery telemanipulator to test sensing of organic tissue on a small scale (see Figure 1). The sensor could gather information about tissue to provide a surgeon tactile feedback via a tactile stimulator. Research into tactile feedback and telesurgical manipulation [Cohn/Lam/Fearing 92],[Cohn/Crawford/Wendlandt/Sastry 95] has made progress. We would like to integrate the microsensor into similar systems. Another use could be placement

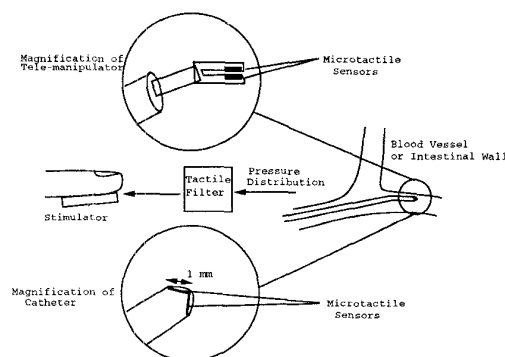


Figure 1: Tactile Feedback From Microsensors

on the fingers of small manipulators other than those designed for surgery.

Potential uses require that the tactile array be 1) small in size (less than 1mm square); 2) inexpensive and disposable for biomedical applications; 3) easily and repeatably mass fabricated in different array sizes; 4) packaged in a useful manner. To meet the first three requirements, we chose a foundry surface micromachining process performed at the MCNC Center for Microelectronics [MCNC 94]. This process consists mainly of two structural layers of polysilicon (poly1 and poly2) and two layers of sacrificial phosphosilicate glass (PSG1 and PSG2). One or both layers of "sacrificial" glass are etched away from the multi-layered process to leave the poly1 and poly2 structural layers free standing (Figure 3). The MCNC process is compatible with IC fabrication, so that a fully integrated sensor could eventually be realized.

2 Sensor Design

2.1 Mechanics of Cell Design

Most macroscopic capacitive tactile sensors are composed of flat, parallel plates separated by a high dielectric elastic material. This is difficult to do on the microscale. Conducting beams are easily fabricated using micro-machining techniques, but have a nonlinear response for larger loads, although it can be approximated as linear for small (less than 10% saturation) pressures.

Polyimide and other layers easily applied using IC processing are not elastic enough for our applications.

*This work was funded in part by: NSF-PYI grant IRI-9157051 and an NSF Graduate Fellowship while B.L. Gray was at the University of California, Berkeley, Dept. of EECS.

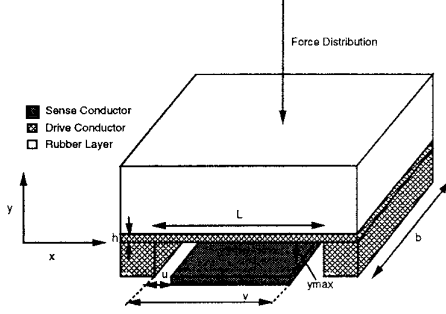


Figure 2: Stylized Model of Cell Showing Variables

Air would seem to be the most attractive dielectric for use between the drive and sensor lines of our array. This conclusion has been reached by other researchers [Suzuki/Najafi/Wise 90], [Wolffenbuttel 94].

A stylized model of our sensor cell, showing physical dimensions, is shown in Figure 2. The drive conductor is modelled as a rigidly supported beam suspended over a flat sense line. We can assume that a signal applied to the rubber surface will be low-pass filtered enough that the force distribution directly on the drive beam will be uniform.

The equation for beam length given a known maximum deflection and uniform pressure on the beam surface is [Shigley/Mitchell 83]:

$$L = \left(\frac{384 y_{max} EI}{pb} \right)^{1/4} \quad (1)$$

Here $E=160\text{GPa}$ for polysilicon, p is the largest detectable pressure before saturating the sensor, and I is the moment of inertia for the beam. The values $h=1.5\mu\text{m}$ and $y_{max}=0.5\mu\text{m}$ are set by the MCNC process. For a doubly-supported beam of width $b=90\mu\text{m}$ and a maximum pressure of 200kPa , a reasonable pressure to exert on organic tissue without tearing or injury, we have a beam length of $L=80\mu\text{m}$.

The vertical deflection, y , of the beam, as a function of horizontal position, x , is:

$$y(x, p) = -\frac{pb}{24IE} x^2 (L - x)^2 \quad (2)$$

The model assumes no tensile or compressive gradient in the polysilicon film. The model also assumes highly stiff step-up supports, which may or may not be an accurate model [Meng/Mehregany/Mullen 93]. However, this basic model should give us an approximate relationship between applied pressure and deflection.

2.2 Electrical Design

To calculate the capacitance between the poly 1 flat conductor and the poly 2 beam under load, we approximate the beam as many parallel plate capacitors of small length and width b . This assumption is reasonable given sensor geometry under pressures less

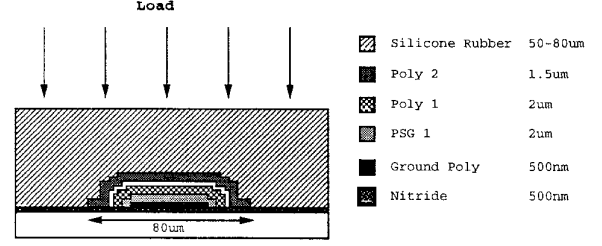


Figure 3: Single Capacitive Tactel

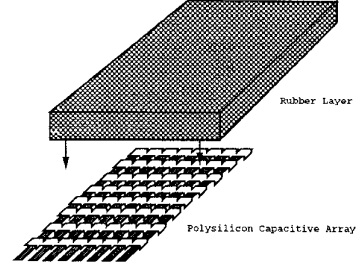


Figure 4: Simplified Illustration of Array

than $0.1p_{max}$. The capacitance of the beam electrode suspended over the flat conductive plate is expressed as:

$$C(p) = \epsilon_0 b \int_u^v \frac{dx}{y_{max} + y(x, p)} \quad (3)$$

where ϵ_0 is the dielectric constant for air, $y(x, p)$ is given in (2), and $v - u = 70\mu\text{m}$. The capacitance is nearly linear for pressures below 20kPa .

The capacitive tactel design is shown in Figure 3. Each cell is composed of a poly0 ground line (to decrease stray capacitance through the substrate), separated from the poly1 sense line by a $2\mu\text{m}$ thick PSG layer. Once the sensors are released, a $0.5\mu\text{m}$ air gap exists between the sense lines and the poly2 drive lines, which run perpendicular to the sense lines with supports between each cell (see Figure 4). Finally, a layer of rubber protects the polysilicon surface and low-pass filters the applied signal. A rubber thickness approximately equal to sensor spacing is a good compromise between sensitivity and aliasing requirements [Fearing 90]. Our rubber layers are slightly thinner since initial experimentation showed that high sensitivity was more difficult to obtain than good interpolation.

Figure 5 shows a scanning electron micrograph of micro-tactels. Figure 6 is a microscope photo of an entire array before rubber application.

3 Analysis

3.1 Predicted Sensitivity

An approximate relationship between change in pressure and change in capacitance is found using the first two terms of the Taylor Series expansion of (3)

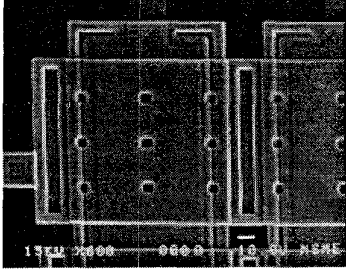


Figure 5: SEM of Two Microtactels: Top View

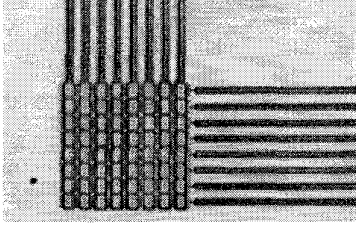


Figure 6: Microscope Photo of Entire 1mm^2 Array Prior to Rubber Application

about the point $p_0=0$:

$$C_s(p) \approx C(p_0) + \frac{\partial}{\partial p}(C(p)|_{p_0})(p-p_0) = C_0 + \Delta C \quad (4)$$

The sensitivity is the derivative term, with the following closed-form solution:

$$S = \frac{\partial}{\partial p} C(p)|_{p_0} = \frac{e_0 b^2}{24 I E y_{max}^2} \left(\frac{x^5}{5} - \frac{L x^4}{2} + \frac{L^2 x^3}{3} \right) \Big|_{x=u}^{x=v} \quad (5)$$

After substitution of numerical values, we obtain an expected sensitivity of $3 \times 10^{-19} \text{F/Pa}$.

Our capacitive sensing technology [Nicolson 94] has a standard deviation of about $5 \times 10^{-17} \text{F}$ at 200kHz bandwidth. Thus, the estimated sensitivity (2σ) is $\delta C = 1 \times 10^{-16} \text{F}$, or 300Pa, or $3 \times 10^{-6} \text{N}$. For comparison, a pressure sensor with similar geometries designed by [Kung/Lee 92] was capable of detecting $3 \times 10^{-17} \text{F}$ capacitance change with on-chip electronics. Our force sensitivity is very high for a tactile sensor, and is compatible with sub-millimeter scale manipulation.

3.2 Predicted Change in Capacitance

Figure 7 shows the electrical model of the capacitor detection circuitry. The voltage output of the tactile sensor can be expressed as $|V_s| = \omega C_s R_1 |V_d|$, where V_d is the drive voltage and C_s is the sensed capacitance. The drive signal frequency is 200kHz. Note that the sensed voltage is proportional to the capacitance.

Percent change in signal can be expressed as:

$$\frac{C_s - C_0}{C_s} \approx \frac{\Delta C}{C_0} = \frac{b \left(\frac{x^5}{5} - \frac{L x^4}{2} + \frac{L^2 x^3}{3} \right) \Big|_u^v}{24 L_c I E y_{max}} \Delta p = K \Delta p \quad (6)$$

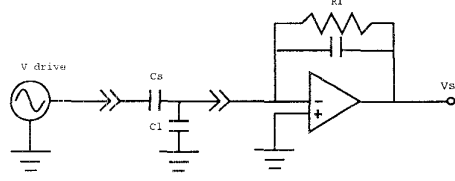


Figure 7: Schematic of Capacitor Detection Circuit

where $\Delta p = (p - p_0)$. Although the expression for the constant K is somewhat complicated, it relies entirely on physical quantities, such as sensor geometries and sensor material. Thus, the microtactile sensor measures change in pressure, rather than the subsurface strain measured by the macroscopic sensor described in [Fearing 90].

3.3 Stability Under DC and AC Signal

A potential problem with capacitive air gap sensors is pull-in under DC bias, where the electrostatic force pulling together the plates is larger than the restoring forces. With micromachined polysilicon plates, this is particularly detrimental since irreparable stiction [Anderson/Colgate 91] or welding of the plates [Chu/Pister 94] may result.

For our tactels, the restoring force is the spring force associated with bending the drive conductor:

$$F_b = \frac{284 I E (y_{max} - y_{gap})}{L^3} \quad (7)$$

where y_{gap} is the distance between conductors at the center of the structure.

The electrostatic force can be solved for numerically using the stored energy in the capacitor:

$$F_{es} = \frac{-\partial U}{\partial y} = \frac{-\partial(\frac{1}{2} C V^2)}{\partial y} = \frac{-V^2}{2} \frac{\partial C}{\partial y} \quad (8)$$

where V is the applied DC bias, and C is found using (3) for values of pressure obtained by varying y_{gap} in (1). An upper bound is set by solving for force as a function of voltage for a parallel plate capacitor separated by the distance y_{gap} :

$$F_{es} = \frac{-V^2 \epsilon_0 b L}{2 y_{gap}^2} \quad (9)$$

The spring force for the beam, and the electrostatic forces for both the beam and parallel plate approximations, are shown in Figure 8. We see that gaps less than 35nm must be avoided. This deflection corresponds to an applied pressure of 196kPa, well above the linear region of 20kPa, indicating stability during normal use.

The minimum DC bias for which pull-in will occur over the entire $0.5 \mu\text{m}$ air gap, using (9), is 45V. From the beam approximation of equation (8), we predict a pull-in of around 70V.

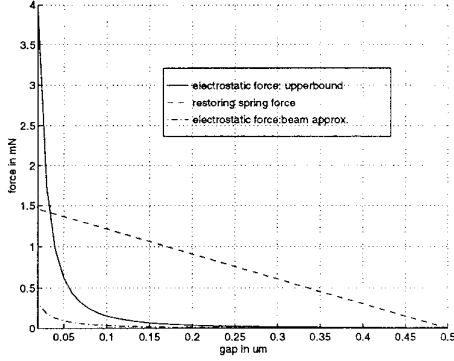


Figure 8: Stability of Sensor Cell Under 7V DC Bias

4 Experimental Results

The sensors were released from the sacrificial PSG2 layer using HF etching. The rubber was molded into thin sheets between glass plates, cut into 1-2 mm^2 pieces, and applied to the released sensor surface while structurally stable, but not completely cured. Removal of the rubber pieces after curing resulted in 60-80% liftoff of the poly2 surface with little damage to the poly1 surface, indicating partial adhesion of rubber to poly2.

The sensor was packaged in a DIP package and placed directly atop the pre-amplification circuitry to minimize pick-up and amplification of stray capacitance. The entire board was placed on a motorized x-y stage accurate to within $1.2\mu\text{m}$. The stage was placed under a microscope for visual inspection.

Two sensors were tested. Sensor A was used for uncoated and rubber-coated static loading tests, and hysteresis measurements. Sensor B was used for spatial impulse response tests and imaging. The major difference between the sensors were the rubber layers, which came from different batches, and may have polymerized slightly differently. The rubber layers also differed in thickness, approximately $50\mu\text{m}$ thick for sensor A and approximately $80\mu\text{m}$ thick for sensor B.

All testing was accomplished using a personal computer and software designed for arrays of larger (3mm spacing) tactile sensors.

4.1 Sensitivity Measurements

4.1.1 Without Rubber, Single Cell

Jewel-bearing meter movements and flat, approximately $80\mu\text{m}$ diameter probe tips were used to apply force directly to the polysilicon surface of the drive lines. The force was increased in steps and the resulting percent changes from baseline capacitance obtained. Figure 9 shows the results of one test, along with a plot of expected values and a linear least-squares fit to the data.

The response is monotonic, but not perfectly linear, with these small forces easily detectable (larger than $0.1\%\Delta C/C_0$). The measured values show sensors that have a somewhat lower sensitivity ($0.022\%\Delta C/C_0/\mu\text{N}$) than predicted ($0.040\%\Delta C/C_0/\mu\text{N}$).

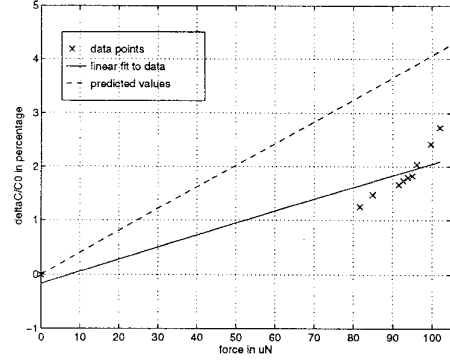


Figure 9: Static Loading: Sensor A Without Rubber

It is possible that either the force application method or the sensor response are nonlinear. In fact, a second order least-squares fit to the data was closer than a linear fit. It is also possible that the force application has large errors in calibration and/or repeatability. We suspect the force application is at fault, since the rubber-coated sensors suggest a fairly linear response. The force range tested is also very small ($20\mu\text{N}$). Still, these experiments show sensors that are behaving at least in the range of what was expected.

The pull-in voltage was determined experimentally for several 200kPa and 100kPa sensor cells. The setup consisted of a high-voltage power supply connected through a $100\text{K}\Omega$ resistor to a sensor cell. A digital storage oscilloscope measured average (over three cells) pull-in voltages of 59V for the 200kPa sensor and 26V for the 100kPa sensor. These measurements are lower than the predicted values of 70V and 55V. They are, however, above the minimum predicted pull-in, using the parallel plate approximation, of 45V and 20V.

No proximity effects or hysteresis effects were noticed, and the post-test and pre-test offset values were virtually the same, indicating recovery of deflected elements under normal operation.

4.1.2 With Rubber, Single Cell

The application of rubber presents many problems to finding a simple sensitivity relationship between pressure on the rubber surface and percent change in capacitance. The elastic behavior of the rubber, the imperfect interface and adhesion between the rubber and the polysilicon, and the low-pass filtering and loss of signal at the polysilicon supports are just a few of the difficulties. We know that sensitivity will diminish, but we cannot easily predict how much it will decrease.

Using a mechanical force gauge and an $80\mu\text{m}$ probe tip, forces were applied in approximately 0.1mN steps to three different sensor cells. The results of this experiment for tactels (4,4), (4,6), and (7,6) are shown on the same axis in Figure 10, along with linear least-squares fits for each cell's data.

The responses were nearly linear for all three cells,

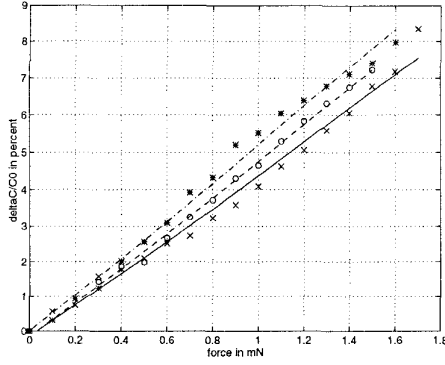


Figure 10: Static Loading: Sensor A with Rubber

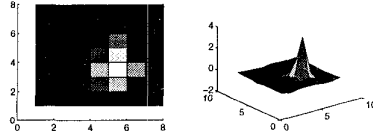


Figure 11: Response to 80 μ m Probe Tip

and we see reasonable consistency between cells. The average sensitivity was $0.005 \text{ } \Delta C/C_0/\mu\text{N}$, or $0.036 \text{ } \Delta C/C_0/\text{KPa}$. Using $0.1 \text{ } \Delta C/C_0$ as the minimum easily detected signal, the minimum detectable force and pressure should be $20\mu\text{N}$ and 2.3kPa , respectively.

4.2 Spatial Impulse Response

The spatial response of a tactile sensor is one of the most important measurements of tactile sensor performance. Because the rubber acts as a low-pass spatial filter, application of a probe to the sensor surface affects not only the tactel(s) directly beneath the probe, but the surrounding tactels as well (see Figure 11). Thus, normal forces can be localized to better than sensor spacing. It is desirable to have spatial uniformity between tactels and enough overlap for good interpolation between elements. It is also desirable to have similar peak deformations for each tactel, i.e.,

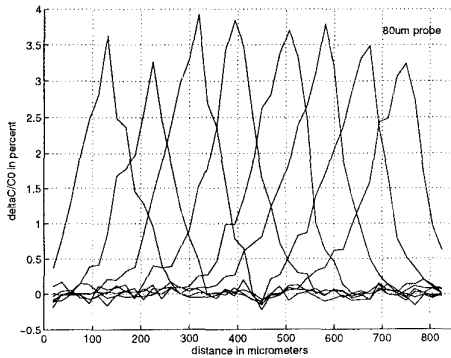


Figure 12: Spatial Impulse Response Test. Response along poly2 to moving probe. Rubber layer:80 μ m.

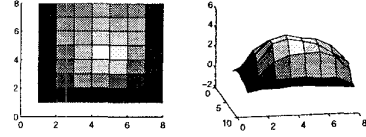


Figure 13: Response to Square Surface Mount Diode

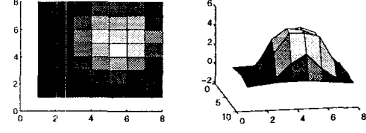


Figure 14: Response to Flat, Circular Probe

uniform gain.

Spatial impulse response tests were performed by stepping the sensor along a line by tens of microns between force applications. The results of one of these tests is shown in Figure 12. For this test, the applied force was approximately 7.5mN using an 80 μ m probe.

The test results are somewhat noisy. We attribute this to the inaccuracies of the testing apparatus. We estimate that the applied force was only repeatable to within 10-20% due to probe slippage, imperfect leveling of the sensor surface, friction in the mechanical gauge, and friction in the probe loading vernier.

Even with such inaccuracies, the overlap is obvious and fairly uniform, as are the peak deformations (gain). Our spatial impulse response tests show much more uniformity in peak sizes than most hand-made, macroscopic capacitive array sensors, where the peak deformations can vary by as much as 3:1 [Sladek/Fearing 90]. This is due to the highly accurate IC processing techniques, with the remaining variation attributed to non-uniformity of rubber thickness and adhesion.

4.3 Qualitative Imaging

We applied various shapes to the sensor surface and plotted the output in gray scale, three dimensions, and using contours (Figures 13 - 15). Although such plots tell us very little about the tactile sensor (Figures 10, 12 and 16 are the real measures), they give us a quick check of qualitative sensor operation.

The razor blade orientation is qualitatively obvious, but the difference between the square and circular objects are not easily seen, although the sensor faithfully reproduced the relative sizes of the objects.

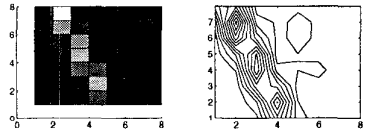


Figure 15: Response to Razor Edge

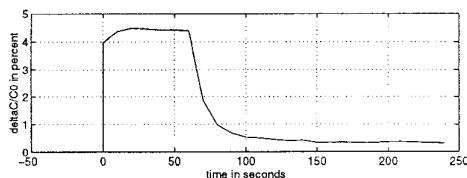


Figure 16: Temporal Response of Rubber-Coated Sensor A, element(2,5)

4.4 Temporal Hysteresis

Hysteresis is the worst problem with our sensors and renders them impractical for applications at present. Whenever an elastomer is used as a structural element and deformed by large amounts, hysteresis results due to elastic set and creep. This has been demonstrated for macroscopic sensors [Sladek/Fearing 90], including human skin [Dinnar 70]. However, the hysteresis that our sensors exhibit cannot be attributed to the usual reasons since it is much worse than previously reported hysteresis for macroscopic sensors. Other causes, such as tactel structure, the imperfect polysilicon/rubber interface, water vapor, or imperfect polymerization of rubber on the microscale may be at fault.

Figure 16 shows a worst result hysteresis test. A force was applied via a 1mm steel sphere under 2.5mN load at time zero, and removed at time 60 seconds. We note the initial signal jump to 90% of its peak, the slow leveling to peak value over 20 seconds, and the extremely slow decay after probe removal. The sensor took nearly a minute to decay to 10% of its peak value. This was not expected.

We are working on ways to reduce the hysteresis via drying techniques, different elastomers, and rubber application methods. We believe further research is worthwhile given the otherwise very positive testing results of the sensor.

5 Conclusions

Linear sensitivity for tactels prior to rubber coating was approximately $0.022\%/ \mu N$ as tested with an $80\mu m$ probe, and $4.88\%/mN$ for rubber coated tactels using an $80\mu m$ probe. Sensor B was somewhat less sensitive; several grams of force were needed to produce usable images of the surface mount diode, which is fine for such a hard object, but far too much for organic tissue. The sensors possessed high spatial resolution and good spatial uniformity. Hysteresis was a severe problem, taking almost 60 seconds for the signal to fall to 10% of the peak deflection, and up to 10% remaining for several minutes. The sensors themselves were inexpensive and disposable even though they were foundry-made prototypes (approximately \$5 per sensor). The largest expense for practical application would be the time-consuming calibration and packaging needed for each sensor.

In summary, the sensors were able to survive repeated contacts with the environment over a several

month period. Off-chip electronics simplified the design of the prototype, allowing us to make direct comparisons with well understood macroscopic sensors that use the same electronics. The sensors possessed sensitivities and spatial performance compatible with the detection of small objects of moderate fragility. The tactels were of high density, acting as a microscope for the sense of touch, able to extract very small features and sense very small objects. Hysteresis and packaging issues must be addressed before the sensor can be considered useful for practical applications.

Acknowledgments

We thank Ed Nicolson and Keelan Jennings for developing the PC tactile software and interface.

References

- [1] K. Anderson and J. Colgate. A model of the attachment/detachment cycle of electrostatic micro actuators. *Micromech. Sensors, Actuators, and Systems- ASME*, 32:255-268, 1991.
- [2] P. Chu and K. Pister. Analysis of closed-loop control of parallel-plate electrostatic microgrippers. In *IEEE Int. Conf. Rob. Aut.*, pages 820-825, May 1994.
- [3] M. Cohn, L. Crawford, J. Wendlandt, and S. Sastry. Surgical applications of milli-robotics. *J. of Rob. Systems*, 12(6):401-416, 1995.
- [4] M. Cohn, M. Lam, and R. Fearing. Tactile feedback for teleoperation. *SPIE Telemanip. Tech.*, 1833:240-254, 1992.
- [5] U. Dinnar. A note on the theory of deformation of compressed skin tissues. *Mathematical Biosciences*, 8:71-82, 1970.
- [6] R. Fearing. Tactile sensing mechanisms. *Int. J. Rob. Res.*, 9(3):3-23, 1990.
- [7] B. Gray. A capacitive surface-micromachined microtactile sensor array. M.S. Thesis, University of California, Berkeley, 1995.
- [8] R. Howe. Tactile sensing and control of robotic manipulation. *Advanced Robotics*, 8(3):245-261, 1994.
- [9] J. Kung and H. Lee. An integrated air-gap-capacitor pressure sensor and digital readout with sub-100 attofarad resolution. *J. Micromech. Systems*, 1(3):121-129, 1992.
- [10] MCNC. *MCNC Multi-User MEMS Processes: Introduction and Design Rules*, rev. 3. MCNC, Research Triangle Park, NC, 1994.
- [11] Q. Meng, M. Mehregany, and M. Mullen. Analytical modeling of step-up supports in surface micromachined beams. In *Proc. 7th Int. Conf. Solid-State Sensors and Actuators*, June 1993.
- [12] E. Nicolson. Tactile sensing and control of a planar manipulator. Ph.D. Thesis, University of California, Berkeley, 1994.
- [13] J. Shigley and L. Mitchell. *Mechanical Engineering Design*. McGraw-Hill, New York, 1983.
- [14] E. Sladek and R. Fearing. The dynamic response of a tactile sensor. In *IEEE Int. Conf. Rob. Aut.*, pages 962-967, May 1990.
- [15] K. Suzuki, K. Najafi, and K. Wise. 1024-element high performance silicon tactile imager. *IEEE Trans. Electronic Devices*, ED-37(8):1852-1860, 1990.
- [16] M. Wolfenbuttel. *Surface Micromachined Capacitive Tactile Image Sensor*. Delft University Press, Netherlands, 1994.